Water Research Laboratory

Affordable Coastal Protection Project: Physical Modelling of Concrete Masonry Blocks and Geotextile Sand Containers

By M J Blacka, D Howe and I R Coghlan

Water Research Laboratory

UNSW Australia
School of Civil and Environmental Engineering

**Affordable Coastal Protection Project:
Physical Modelling of Concrete Masonry Blocks and Geotextile
Sand Containers**

WRL Technical Report 2016/24
April 2017

by
M J Blacka, D Howe and I R Coghlan

Project Details

Report Title	Affordable Coastal Protection Project: Physical Modelling of Concrete Masonry Units and Geotextile Sand Containers
Report Author(s)	M J Blacka, D Howe and I R Coghlan
Report No.	2016/24
Report Status	Final
Date of Issue	20 April 2017
WRL Project No.	2016057.01
Project Manager	Matt Blacka
Client Name	Pacific Region Infrastructure Facility
Client Address	C/- Asian Development Bank Level 20, 45 Clarence Street Sydney NSW 2000
Client Contact	Lorena Estigarribia (PRIF), Tom Shand (T+TI)
Client Reference	

Document Status

Version	Reviewed By	Approved By	Date Issued
Draft V 1.0	J T Carley	G P Smith	7th November 2016
Draft V 1.1	J T Carley	G P Smith	21st November 2016
Draft V 2.0	J T Carley	G P Smith	21st February 2017
Final	J T Carley	G P Smith	20th April 2017

A major group within

water@
UNSW
water research centre

bsi. ISO 9001 Quality Management

Contents

List of Tables

List of Figures

Acknowledgements

1.   Introduction

Management of coastal erosion and recession of shorelines is an ongoing challenge for most countries in the Pacific Islands, with causes of erosion varying from location to location but broadly including:

- Storms/cyclones and associated large waves and high water levels;
- Distant generated swell events;
- Changes in sediment budget and movement due to both anthropogenic and natural changes in environmental processes (such as sand mining, coastal development and protection, changes in sediment production from reefs, damming or changes to rivers, etc.;
- Climate change effects such as sea level rise, changes to storm frequency, intensity and distribution, and changes to longer term cycles such as ENSO with its associated impacts on sea levels and storminess.

Tonkin + Taylor International (T+TI) were engaged by the Pacific Region Infrastructure Facility (PRIF) to undertake specialist coastal engineering research on options for coastal protection, with a focus on Pacific Island Countries (PICs). An initial desktop review of existing coastal protection methods used throughout the Pacific was undertaken (PRIF, 2016) and identified the potential to use locally available and/or lower cost materials for coastal protection in low wave energy environments. However, it was also identified that physical model testing was required to provide sufficient design information to inform preparation of generic design guidance for these more affordable coastal protection options.

The Water Research Laboratory (WRL) of the School of Civil and Environmental Engineering at UNSW Sydney was commissioned by the PRIF to undertake the physical model investigations. Specifically, WRL were engaged to undertake wave flume modelling of revetments armoured with:

- Small hand placed geotextile sand containers (GSCs), commonly referred to as "geobags" or "sandbags"; and
- Pattern placed concrete masonry building blocks (CMBs), commonly referred to as "Besser blocks".

This report presents the results of WRL's physical modelling investigation, with the intention of informing the development of subsequent design guidance for these forms of affordable coastal protection.

2. Study Objectives

PRIF (2016) identified the potential viability of GSCs for coastal protection in PICs, in particular for remote or isolated islands where transport costs of construction materials can dominate. The report found that smaller hand-filled and placed units made from high quality geotextile, are likely to be viable for stabilising eroding coasts in lower wave energy areas (such as some sections of lagoon coast on atolls). However, to date the stability of such units under wave attack has yet to be investigated, with most GSC studies focusing on the larger 0.75 m^3 or 2.5 m^3 units that have now been widely used around the world.

PRIF (2016) also identified the potential viability of using commonly available building materials such as CMBs ("Besser" style building blocks) as a substitute for more complex/specialist pattern placed revetment armouring systems, in particular for lower wave energy locations. As with the GSCs, CMBs are able to be hand placed and largely eliminate the requirement for heavy construction equipment to build small-scale coastal protection structures in relatively sheltered areas. Furthermore, they are readily available throughout much of the Pacific, either imported or locally cast.

This study aims to specifically investigate the stability of smaller hand-placed GSCs and CMBs under wave attack, including the effectiveness of a range of placement configurations, using a two-dimensional (2D) wave flume physical scale model. A secondary objective of the study is to investigate other factors influencing the design of coastal protection structures with these materials, such as wave runup coefficients and likely failure mechanisms. Through re-analysis (re-scaling) of the wave flume testing results, the outcomes and design guidance for GSCs are also able to be compared with previous design guidelines for larger GSCs such as Coghlan *et al.* (2009).

3. Two-Dimensional Model Setup and Operation

3.1 Testing Facility

Two-dimensional testing was undertaken in the 1.2 m wave flume at WRL. This flume measures approximately 44 m in length, 1.2 m in width and 1.6 m in depth. The flume walls are primarily constructed of waterproofed concrete masonry blockwork, with the exception of a 12 m long glass panelled section where models are constructed, which allows visual observations to be made throughout testing. The permanent floor of the flume is constructed of concrete, and during the testing undertaken for this study a representative bathymetry profile was constructed in the flume as a raised plywood platform supported by timber framing.

The wave generator in this flume is a paddle type and is powered by a 30 kW hydraulic piston system. The system is capable of generating both monochromatic and irregular wave spectra, with only irregular waves tested in this investigation. The input signal is generated and fed to the wave generator using a PC with a custom developed wave generation software package.

3.2 Model Design and Scaling

3.2.1 General Model Scaling

Model scaling was based on geometric similarity with an undistorted length scale of 1:7.5 used for all tests. The scaling relationship between length and time was determined by Froudian similitude, with the following relevant scale ratios (prototype divided by model) being adopted for the model:

- Length ratio $L_R = 7.50$
- Time ratio $T_R = L_R^{0.5} = 2.74$
- Velocity ratio $V_R = L_R^{0.5} = 2.74$
- Mass ratio $M_R = L_R^3 = 421.88$
- Overtopping ratio $Q_R = L_R^{1.5} = 20.54$

3.2.2 Geotextile Sand Container Scaling Considerations

A key characteristic of the GSCs that were to be tested in this investigation, is that they were intended to be hand-placed. As such, it was considered in the project brief that a GSC mass of 40 kg is a reasonable upper limit to be hand-placed by two people. This mass was used as a basis for the container design. Blacka *et al*. (2007) is the only known investigation to report measurements of the characteristics of full scale GSCs, as such the results of this investigation were used to develop suitable design characteristics for smaller 40 kg GSCs in this investigation.

The 0.75 m^3 Elcorock GSCs considered in Blacka *et al.* (2007) were dry filled (as opposed to hydraulically filled as per larger 2.5 m^3 GSCs), and have been used as a guideline to establish the target proportions for the 40 kg GSCs used in this investigation. Table 3.1 and Figure 3.1 show the characteristics of the 0.75 m^3 measured by Blacka *et al.* (2007) and the corresponding characteristics of the 40 kg GSCs used in this investigation that have been scaled proportionately.

Table 3.1: Characteristics of 0.75 m³ and Proposed 40 kg GSCs

	0.75 m³ GSCs (Measured Properties)	Full Scale 40 kg GSCs (Target Properties)	1:7.5 Scale 40 kg GSCs (Target Properties)
Average Mass[1]	1264 kg	40 kg	95 g
Volume	0.915 m³	0.029 m³	69 cm³
Typical Length, L	1800 mm	570 mm	76 mm
Typical Width, W	1500 mm	474 mm	63 mm
Typical Depth, D	420 mm	133 mm	18 mm

1. GSC mass at ambient moisture content

Figure 3.1: GSC Dimension Diagram (Geofabrics Australasia Pty Ltd)

Two important points were considered in the scaling and selection of a geotextile fabric for the model scale GSCs:

1. The exact geotextile fabric that would be used to produce the full sized 40 kg GSCs is not confirmed and would require further considerations with geotextile suppliers. It would likely be a fabric with similar properties to Texcel 600R or 800R (produced by Geofabrics Australasia) that is presently used for 0.3 m³ and 0.75 m³ GSCs. As such, it is not possible to confirm the exact scaled geotextile properties that the model GSCs were aiming to represent.

2. There is a finite range of geotextile fabrics available to use for fabricating the model scale GSCs. As such it is not possible to exactly match target characteristics but instead a fabric is selected that is considered broadly representative for the purposes of the modelling, and will result in slightly conservative predictions from the modelling.

For construction of the model GSCs, in addition to the obvious geometric scaling it was also necessary to consider other important properties of both the geotextile material and the sand fill. This analysis was previously undertaken by Coghlan *et al.* (2009) for a model scale of 1:8, and so the results are almost directly applicable to this modelling study which has a scale of 1:7.5. After a detailed analysis, Coghlan *et al.* (2009) selected the "FT150" geotextile fabric for production of model GSCs. This fabric was also recommended to be used for this project in the

modelling *Terms of Reference*, due to the very similar modelling scale adopted. As such, the model 40 kg GSCs in this investigation were fabricated using FT150 geotextile fabric.

A detailed analysis of scaling considerations for the geotextile fabric and sand fill material is included in Appendix A.

3.2.3   Concrete Masonry Block Scaling Considerations

As stated above, in Australia concrete masonry blocks are typically referred to as "Besser" blocks. In other countries they are also known as concrete blocks, grey blocks, breeze blocks and cinder blocks. In Australia and New Zealand, the manufacture of concrete masonry blocks is covered under the joint standard AS/NZS 4455:1997. Internationally there are slight variations in details of typical concrete masonry blocks used for construction. In the USA the blocks are fabricated to a modular sizing scheme that is based on imperial units, whereas in Australia and New Zealand (and most of the southern hemisphere) the sizing is based on metric units. For the purposes of this study a metric based block was assumed, with details of the full and model scale blocks shown in Table 3.2 and Figure 3.2.

Table 3.2: Properties of Typical Concrete Masonry Block Used for Project

	Full Scale CMB (Typical Properties)	Model Scale CMB (Target Properties)
Mass	16.9 kg	40 g
Volume	7,622,824 mm^3	18,069 mm^3
Density	2217 kg	2217 kg
Length, L	390 mm	52.0 mm
Width, W	190 mm	25.3 mm
Height, H	190 mm	25.3 mm
Thickness, T1	36 mm	4.8 mm
Thickness, T2	32 mm	4.3 mm
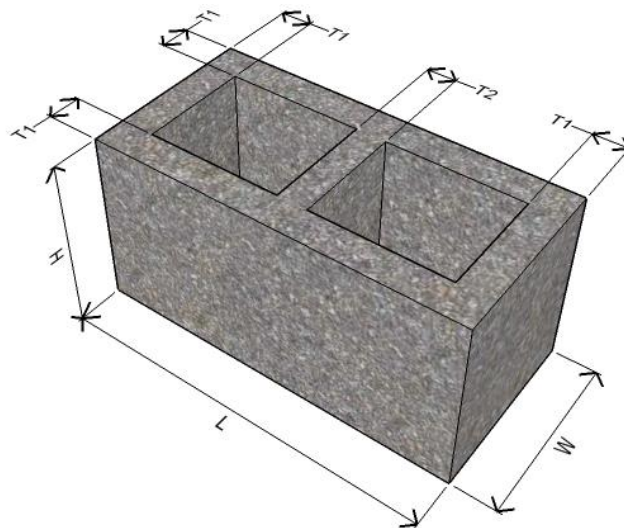
Figure 3.2: Concrete Masonry Block Diagram

Fabrication of the model CMBs was contracted to the specialist plastic injection moulding company Metplas Pty Ltd. A precision mould was developed to accurately cast blocks of the specified dimensions, using a high density plastic.

3.3 Model Construction

3.3.1 Bathymetry

WRL assessed the indicative reef type bathymetric profile suggested in the modelling *Terms of Reference* and found that the slopes were very flat, typically in the range of 1V:200H to 1V:400H. For the purposes of the modelling study it was considered reasonable that such flat bathymetric slopes be simulated in the model as a true flat profile. As the testing was being undertaken to establish design guidance for application on a wide range of potential reef/lagoon bathymetry conditions, simulating an exact profile was also of lower importance for this study. The flat model bathymetry was reproduced in the flume for a distance of approximately 70 m seaward of the test revetment, before transitioning to the flume floor. The bathymetric profile used in the modelling investigation is summarised in Table 3.3.

Table 3.3: Details of Bathymetric Profile

Bathymetric Section	Horizontal Distance Seaward of Test Revetment (m)	Bathymetric Gradient	Bathymetric Depth (m Relative to Revetment Toe)
Nearshore Profile	0 – 70.0 m	Flat	0.0 – 0.0 m
Transition Slope 1	70.0 – 82.1 m	1V:16.8H	0.0 – 0.8 m
Transition Slope 2	82.1 – 91.1 m	1V:2.3H	0.8 – 4.7 m

The bathymetric profile in the wave flume was constructed from hardwood form ply, supported on a timber frame such that deflections under moving waves were negligible.

3.3.2 Test Revetment Structures

To ensure that the modelling results were considered applicable to a wide range of sites and potential revetment applications, the model revetments were constructed with an impermeable structure core that provided a slightly conservative prediction of armour stability. The revetment core was fabricated from hardwood form ply topped with a layer of thin geotextile to create a more realistic interface friction with the armour layers.

Table 3.4 provides a summary of the various revetments tested in the modelling program, with details and drawings of the revetments provided in Section 3.3.2.1 (Concrete Masonry Blocks) and 3.3.2.2 (Geotextile Sand-Filled Containers). All revetment structures were built with a 1V:1.5H slope, as per the modelling *Terms of Reference*.

Table 3.4: Summary of Revetment Configurations Tested

Revetment	Armour Type	Armour Placement	Crest
CMB1	Concrete Masonry Blocks	Long axis shore parallel	Non-overtopped
CMB2	Concrete Masonry Blocks	Long axis shore perpendicular	Non-overtopped
CMB3	Concrete Masonry Blocks	Alternating shore parallel and perpendicular courses	Non-overtopped
CMB4	Concrete Masonry Blocks	Long axis shore parallel	Overtopped
CMB5a *	Concrete Masonry Blocks	Long axis shore parallel, "minor damaged" armour units	Non-overtopped
CMB5b *	Concrete Masonry Blocks	Long axis shore parallel, "significantly damaged" armour units	Non-overtopped
CMB6 *	Concrete Masonry Blocks	Combined long axis shore parallel and "upstand" blocks	Non-overtopped
GSC1	Geotextile Sand-filled Containers	Double layer, long axis shore parallel	Non-overtopped
GSC2	Geotextile Sand-filled Containers	Single layer, long axis shore perpendicular	Non-overtopped
GSC3	Geotextile Sand-filled Containers	Double layer, long axis shore parallel	Overtopped

* Notes: Tests on CMB5 and CMB6 were undertaken as additional tests to the original program

3.3.2.1 Concrete Masonry Block Revetments

As required in the modelling *Terms of Reference*, the concrete masonry block revetments were constructed with a graded rock underlayer/secondary armour layer between the blocks and the revetment core. The rock underlayer had a median stone size (D_{n50}) of 69 mm (full size, real world scale), and was considered a reasonable match for the 75 mm rock size specified in the *Terms of Reference*, as shown in Figure 3.3. The underlayer was placed on the revetment to a thickness of 150 mm as required in the modelling *Terms of Reference*.
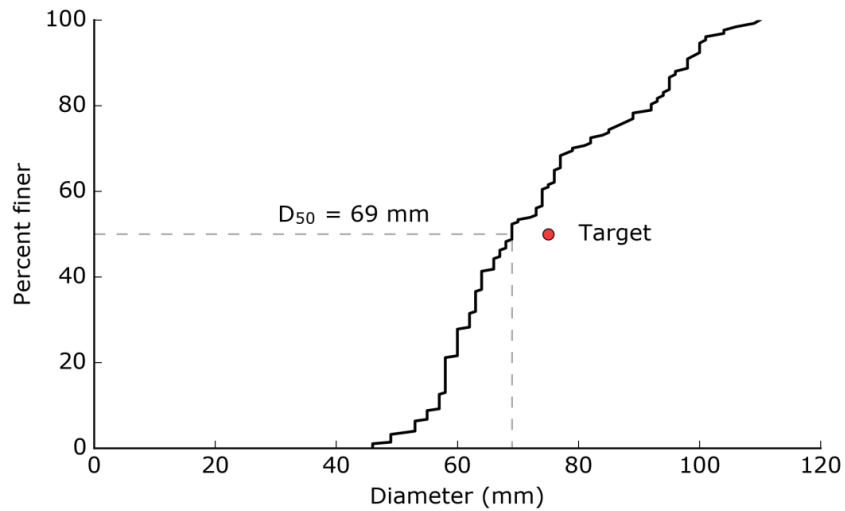
Figure 3.3: Secondary Armour Grading Curve for Concrete Masonry Block Revetments

Four (4) different CMB revetment designs were tested in the initial flume modelling program, with details summarised in Table 3.4 and Figure 3.4 to Figure 3.7. The revetment designs included three (3) non-overtopped revetments used to investigate the stability of CMBs in three different placement patterns on the revetment slope, as well as one (1) overtopped revetment used to investigate the stability of CMBs on the revetment crest under overtopping flows.

An additional range of tests were also undertaken as a variation to the original scope, and investigated the influence of damaged armour units on armour stability (Figure 3.8 and Figure 3.9), as well as the influence on an "upstand" block arrangement on wave runup (Figure 3.10).
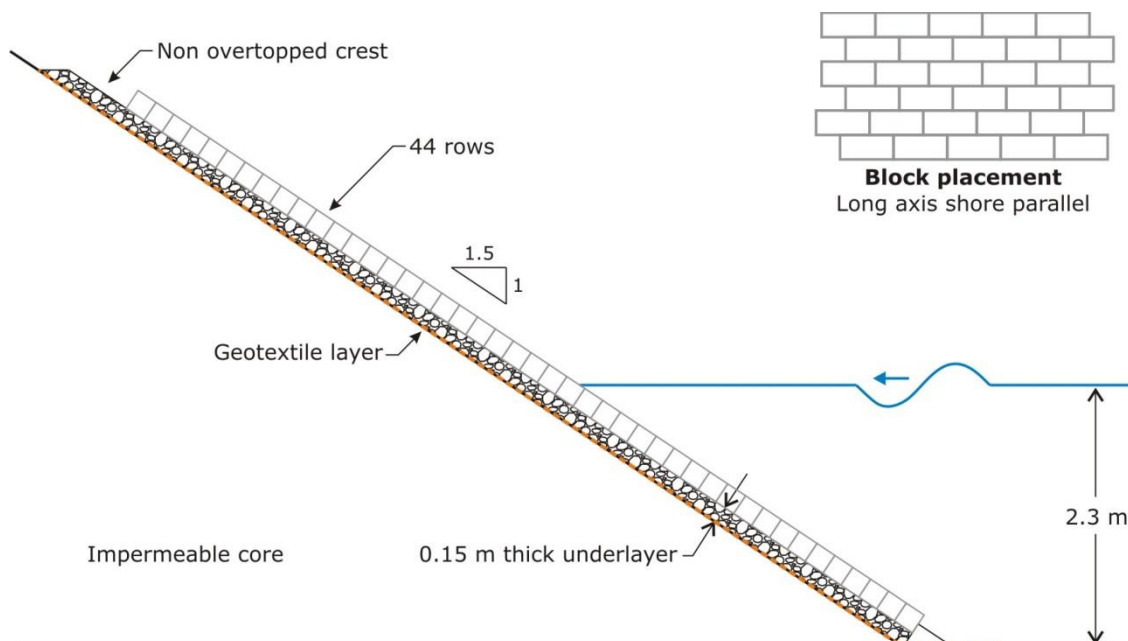
Figure 3.4: Revetment Design CMB1
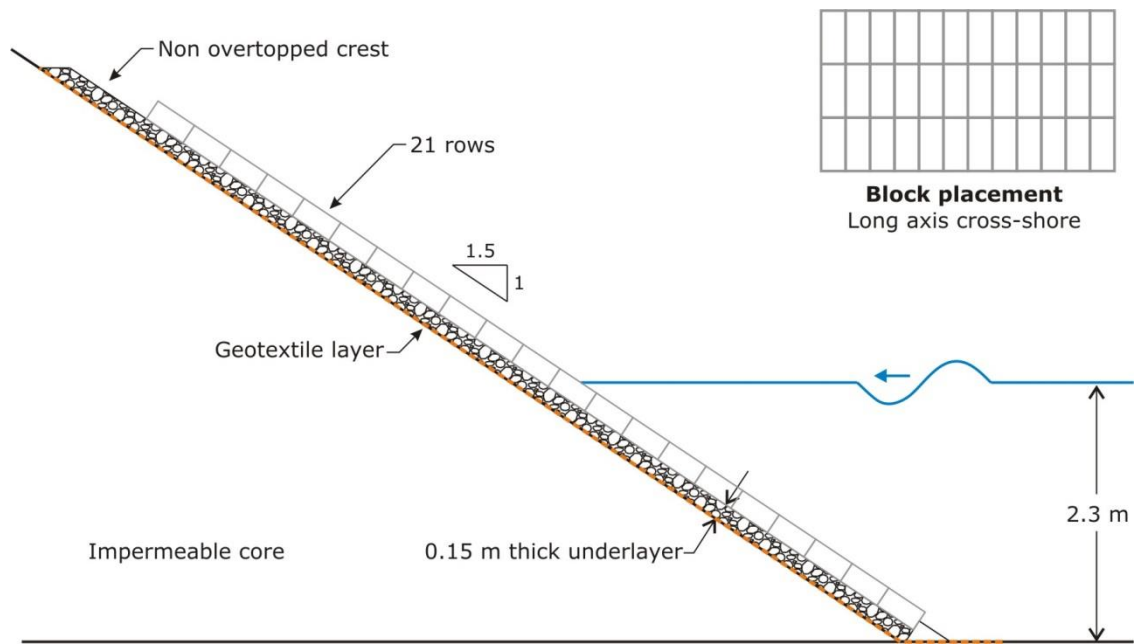
Figure 3.5: Revetment Design CMB2

Figure 3.6: Revetment Design CMB3
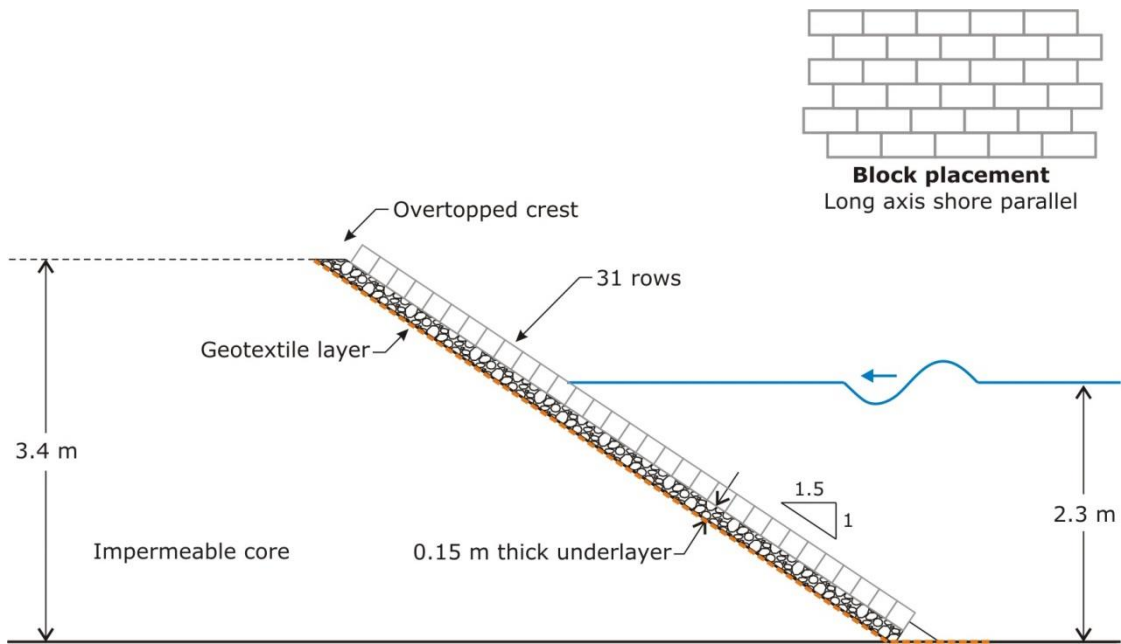
Figure 3.7: Revetment Design CMB4
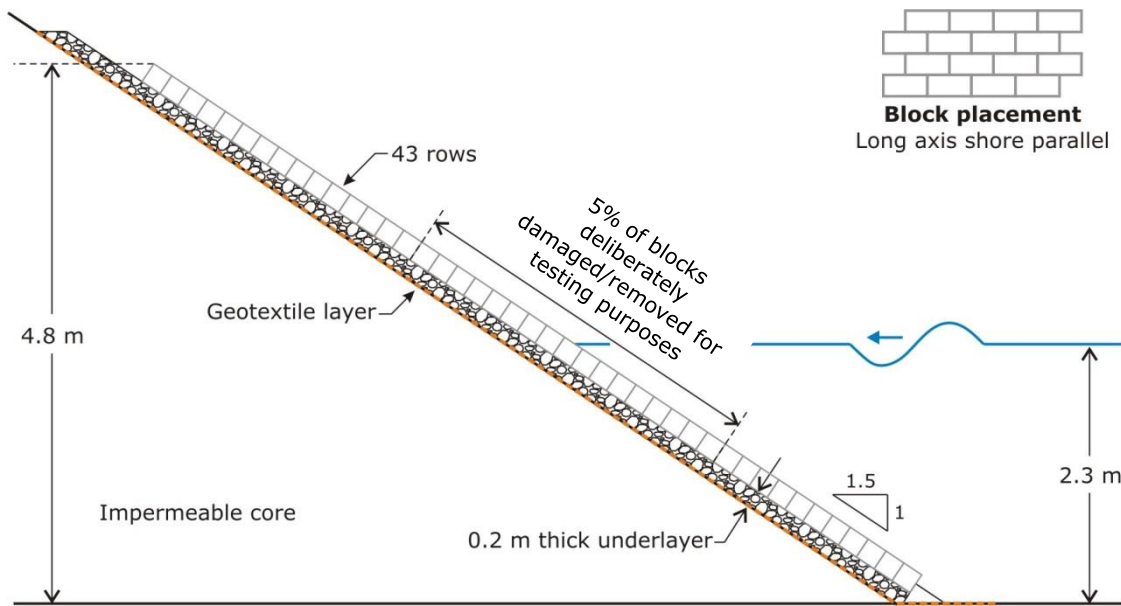
Figure 3.8: Revetment Design CMB5a
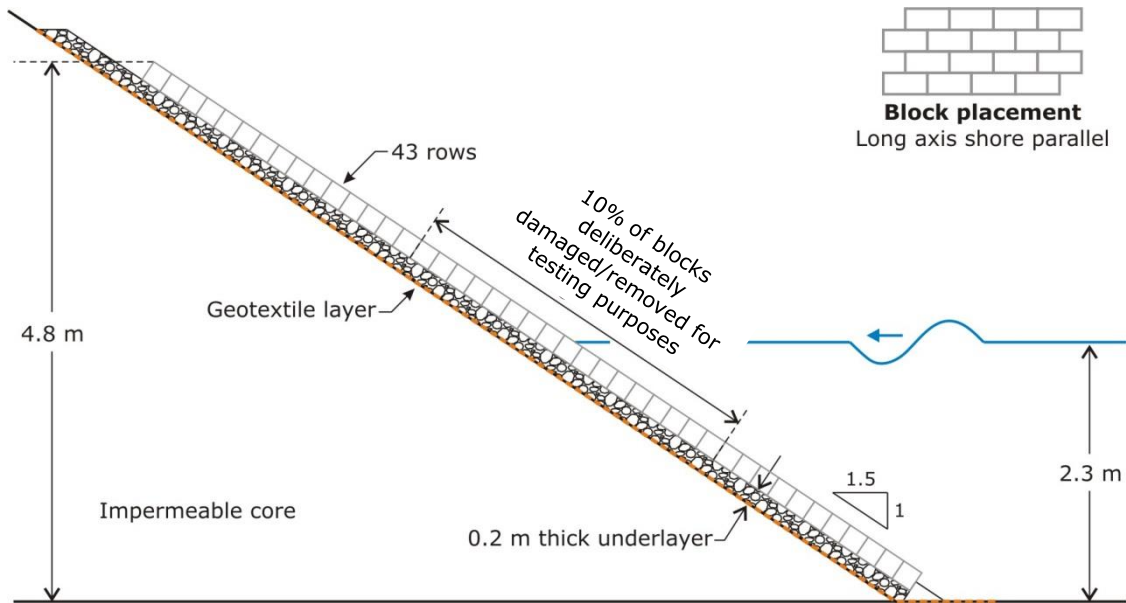
Figure 3.9: Revetment Design CMB5b
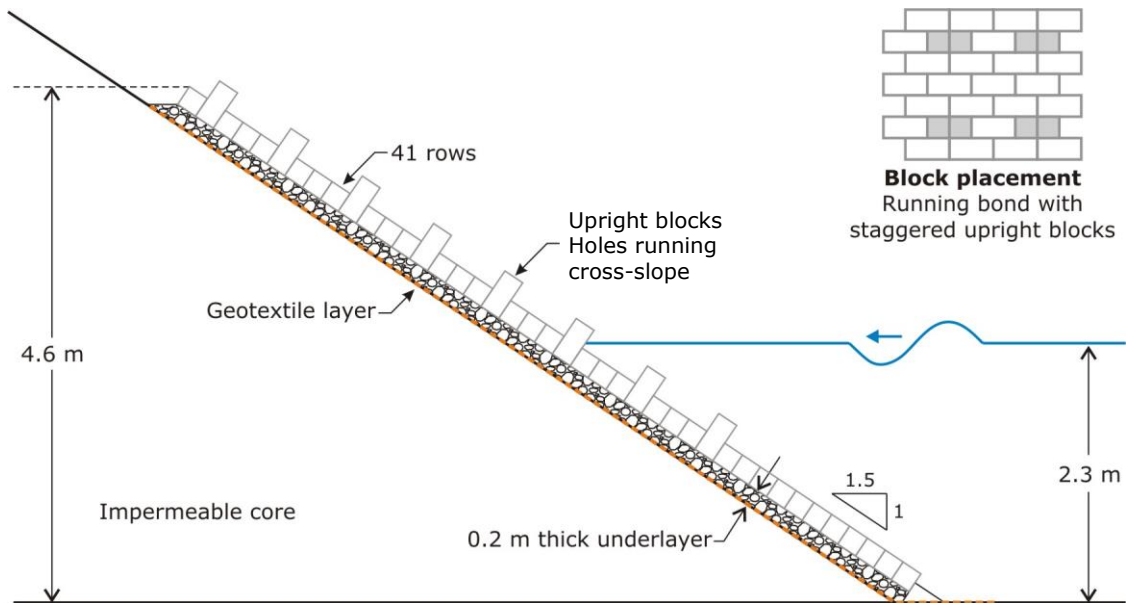
Figure 3.10: Revetment Design CMB6

3.3.2.2 Geotextile Sand-Filled Container Revetments

As outlined in the modelling *Terms of Reference* (and discussed in Appendix A), the model geotextile sand-filled containers were fabricated from FT150 geotextile so as to achieve bag properties that resembled full scale containers as closely as possible. Prior to mass production of the model GSCs, a number of fabric shapes were initially trialled to investigate the resulting bag shape that was produced when full. Once the required shape was achieved, cutting and stitching of the model bags was undertaken by a contracted upholsterer.

The model bags were filled with fine-grained marine sand sourced from Anna Bay on the NSW mid-north coast, so that the permeability of the fill material followed the required scaling parameters (see Appendix A and B). A fixed-volume filling container was fabricated that held the required mass of sand when filled, and was used throughout the bag filling process to ensure that the bags had a consistent mass of fill material. This technique resulted in model GSCs that had a low variation in mass, typically of the order of +/- 3% of the target GSC mass.

Three different GSC revetment designs were tested in the flume modelling program, with details summarised in Table 3.4 and Figure 3.11 to Figure 3.13. The revetment designs included two non-overtopped revetments used to investigate the stability of GSCs in two (2) different placement patterns on the revetment slope, as well as one (1) overtopped revetment used to investigate the stability of GSCs on the revetment crest under overtopping flows.
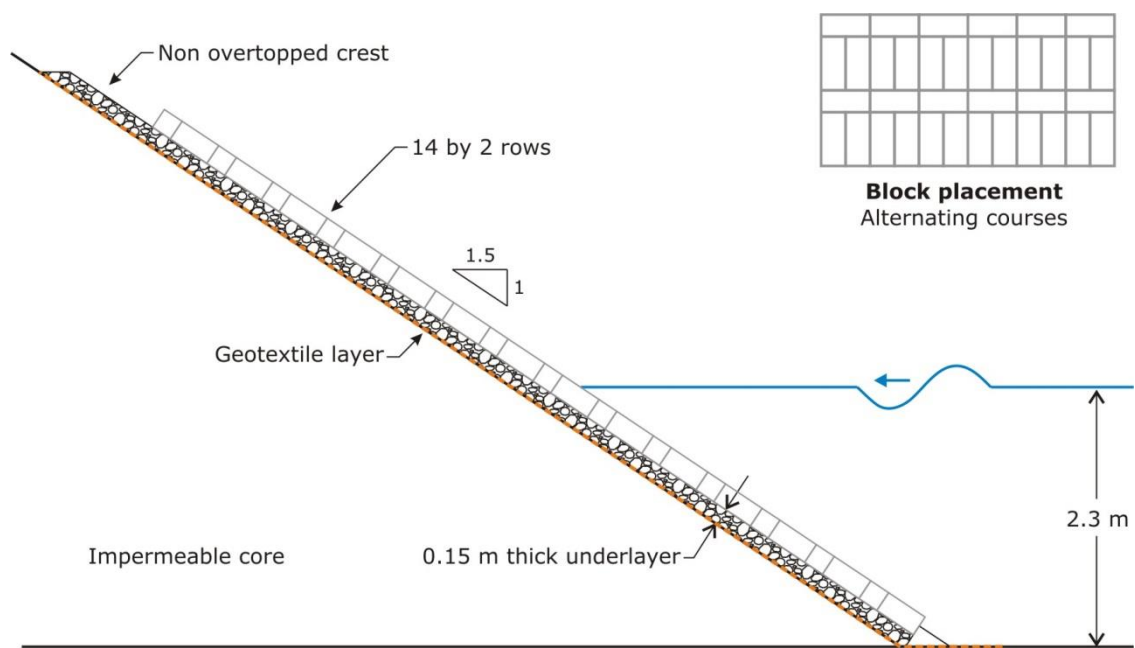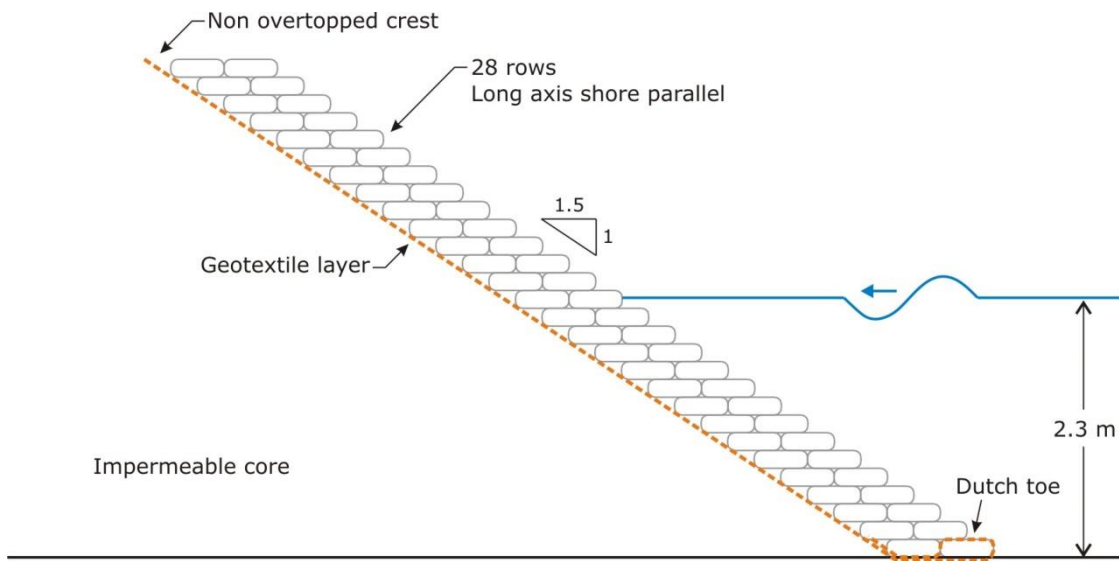

Figure 3.11: Revetment Design GSC1
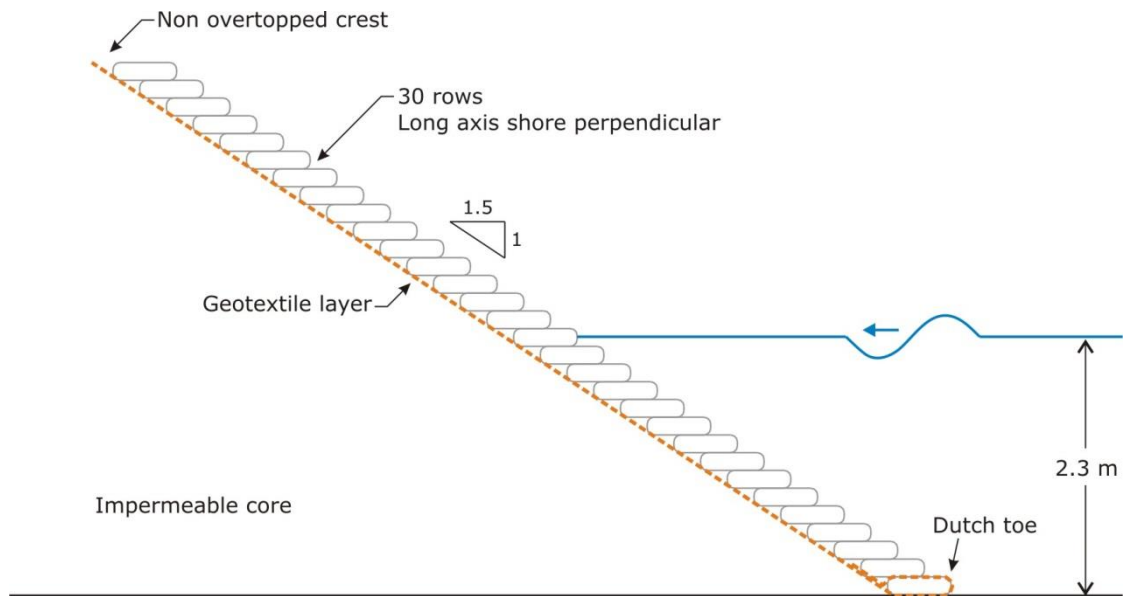
Figure 3.12: Revetment Design GSC2
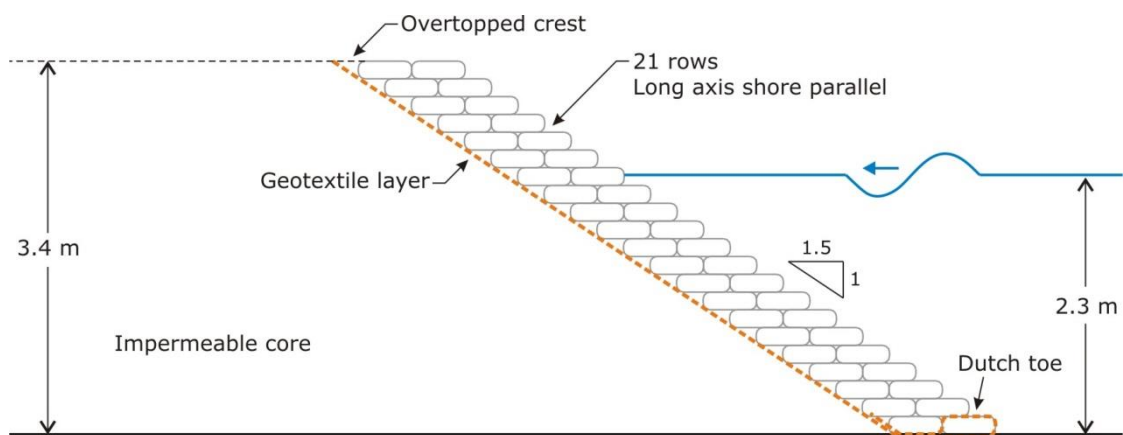
Figure 3.13: Revetment Design GSC3

3.4 Data Collection Methods

3.4.1 Wave Records

Wave conditions were measured continuously throughout all tests at two (2) locations in the wave flume, using arrays that each contained three high accuracy capacitance wave gauges. The wave conditions presented in this report are from a gauging location that was just seaward of the test revetment. Data from the individual wave probe records was analysed using the least squares method of Mansard and Funke (1980) to separate incident and reflected waves. Incident wave statistics (with the effect of reflected waves removed) recorded at the measurement location have been provided for each test.

3.4.2 Runup and Overtopping Measurements

Runup levels were measured continuously throughout most tests using a capacitance wave gauge mounted along the revetment face. Data from this gauge was post-processed to estimate the runup level that was exceeded by the largest 2% of wave runups ($R_{u2\%}$), and reported for each test.

Overtopping was measured throughout a small number of tests using a time-averaged volumetric method. Any wave overtopping flows passing over the crest of the revetment throughout a test were captured and totalled, to allow for an estimation of the average wave overtopping rate throughout the test.

3.4.3 Concrete Masonry Block and Geotextile Sand-Filled Container Damage Assessment

Stability of the CMBs and GSCs was monitored through all tests using a combination of visual observations, pre and post-test photographs, as well as video records. Typically, observations were used to identify when damage to a revetment was initiated, and if the damage was progressive towards failure with ongoing wave attack.

4. Test Program Summary

The overall objective of the testing program was to investigate the stability of both the GSC and CMB revetments under a range of wave conditions expected to be experienced on low-energy coastlines of Pacific Islands, to determine the upper limit of wave conditions where these revetment types could be applied.

A range of wave conditions were investigated, with three different wave periods (3 s, 5 s and 10 s) and wave heights up to either:

- The wave height that resulted in significant damage or failure of the revetment;
- The physical steepness or depth limit of waves at which higher waves would break prior to reaching the test structure; or
- The limit of the wave machine.

In order to minimise test permutations, not all wave period and wave height combinations were tested where it was very unlikely that any damage to a test revetment would occur. Instead the testing program was targeted at identifying the threshold of wave conditions at which point damage to the revetment would begin to occur. All tests were undertaken with a water depth of 2.3 m at the revetment toe, which was considered a suitable depth to achieve the target range of potential wave conditions and was also considered realistic for the potential application locations.

Table 4.1 and Table 4.2 provide a summary of the test permutations undertaken for the CMB and GSC revetments respectively, as part of the original testing program.

Table 4.1: Summary of Concrete Masonry Block Test Program

Revetment Reference	Armouring	Wave Period, T_p (s)	Wave Height Range H	Test Purpose
CMB1	Long axis shore parallel	3	Up to steepness limited waves (max $H_s \sim 0.9$ m)	Slope armour stability
		5	Up to depth limited waves (max $H_s \sim 1.1$ m)	Slope armour stability
		10	Up to wave machine capacity (max $H_s \sim 0.9$ m)	Slope armour stability
CMB2	Long axis shore perpendicular	3	Up to steepness limited waves (max $H_s \sim 0.9$ m)	Slope armour stability
		5	Up to depth limited waves (max $H_s \sim 1.1$ m)	Slope armour stability
		10	Up to wave machine capacity (max $H_s \sim 0.9$ m)	Slope armour stability
CMB3	Alternating courses of shore parallel and shore perpendicular	3	Up to steepness limited waves (max $H_s \sim 0.9$ m)	Slope armour stability
		5	Up to depth limited waves (max $H_s \sim 1.1$ m)	Slope armour stability
		10	Up to wave machine capacity (max $H_s \sim 0.9$ m)	Slope armour stability
CMB4	Long axis shore parallel	5	Up to crest failure	Crest armour stability

Table 4.2: Summary of Geotextile Sand-Filled Container Test Program

Revetment Reference	Armouring	Wave Period, T_p (s)	Wave Height Range H	Purpose
GSC1	Double layer, long axis shore parallel	3	Up to structure failure (max H_s = 0.4 m)	Slope armour stability
		5	Up to structure failure (max H_s = 0.6 m)	Slope armour stability
		10	Up to structure failure (max H_s = 0.7 m)	Slope armour stability
GSC2	Single layer, long axis shore perpendicular	3	Up to structure failure (max H_s = 0.5 m)	Slope armour stability
		5	Up to structure failure (max H_s = 0.7 m)	Slope armour stability
		10	Up to structure failure (max H_s = 0.7 m)	Slope armour stability
GSC3	Double layer, long axis shore parallel	5	Beyond structure slope capacity (max H_s = 0.9 m)	Crest armour stability

Following the completion of the original testing program, it was decided that further testing of the CMB revetments should be undertaken to investigate:

- The influence of damaged blocks on the overall stability of the armour layer (given that some degree of block breakage can be expected during large storms);
- The influence of an alternative block placement pattern having some blocks stood on end ("upstand") so as to reduce wave runup.

Table 4.3 provides a summary of the test permutations undertaken for these additional CMB revetments.

Table 4.3: Summary of Additional Concrete Masonry Block Tests

Revetment Reference	Armouring	Wave Period, T_p (s)	Wave Height Range H	Test Purpose
CMB5a	Long axis shore parallel (minor damage to block layer)	5	Up to steepness limited waves (max H_s ~ 1.1 m)	Slope armour stability with minor damage to armour layer
CMB5a	Long axis shore parallel (minor damage to block layer)	5	Up to steepness limited waves (max H_s ~ 1.1 m)	Slope armour stability with significant damage to armour layer
CMB6	Long axis shore parallel with upstand blocks	5	Up to steepness limited waves (max H_s ~ 1.1 m)	Wave runup reduction with upstand blocks

5. Concrete Masonry Block Testing Results

5.1 CMB Slope Armour Stability Characteristics

5.1.1 General Slope Armour Stability

Non-overtopped revetments constructed with three (3) different CMB placement patterns were each tested for wave periods (T_p) of 3, 5 and 10 seconds. The revetments were exposed to wave conditions with significant wave height up to the maximum possible for each wave period, in order to assess the stability of the CMBs on the revetment slope. The limiting factor on wave heights tested varied for each wave period as:

- 3 second period waves were limited by maximum wave steepness;
- 5 second period waves were depth limited by the bathymetry;
- 10 second waves were limited by the capacity of the wave machine.

Under all tested conditions for all three block placement configurations, the concrete masonry blocks on the revetment slope were observed to be completely stable with no block displacement or movement. There was also no displacement of the 70 mm underlayer rock through the holes in the CMBs. These stability results are summarised in Figure 5.1 to Figure 5.3. Tabulated test result data is provided in Appendix C.
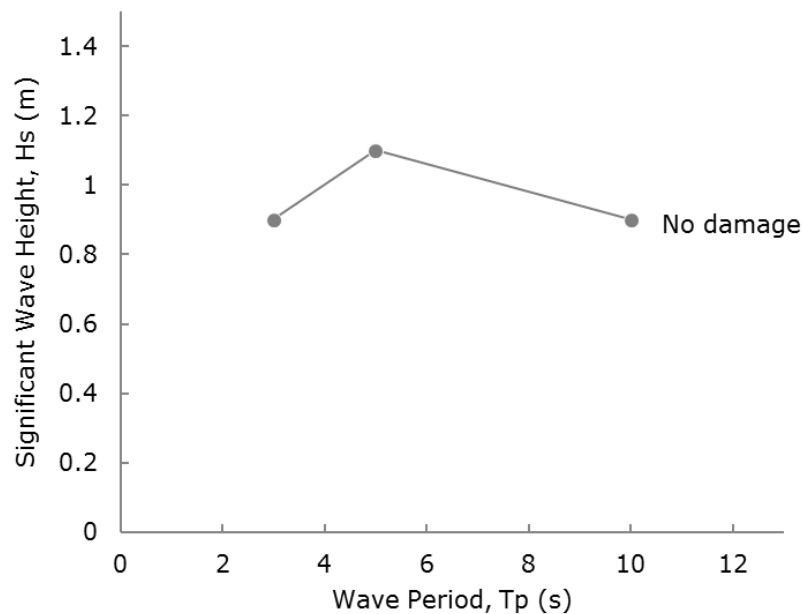
Figure 5.1: CMB1 Revetment Stability Results
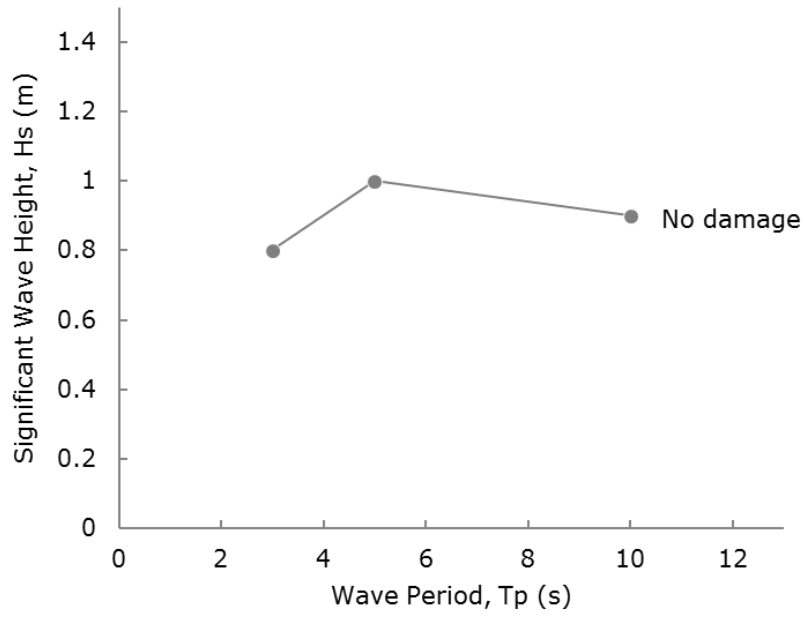
Figure 5.2: CMB2 Revetment Stability Results
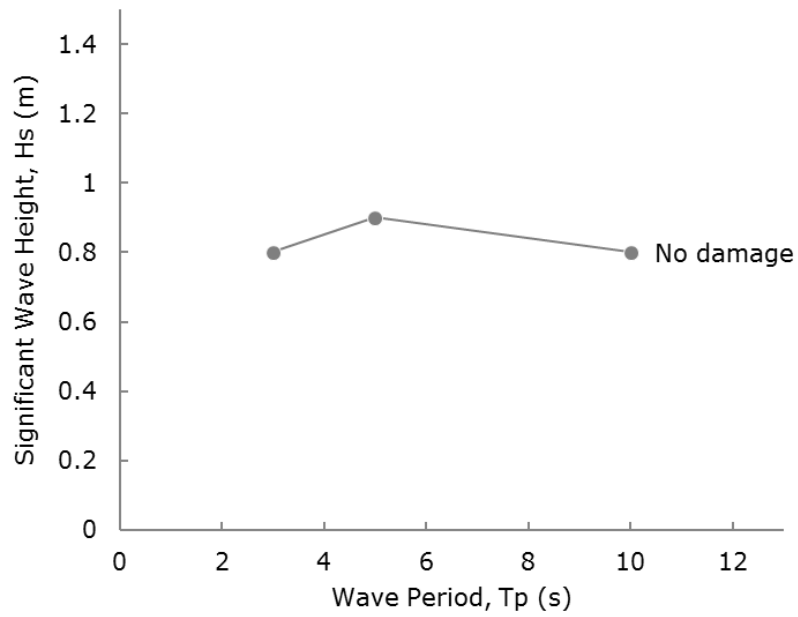
Figure 5.3: CMB3 Revetment Stability Results

5.1.2 Damaged Slope Armour Stability

A non-overtopped revetment was constructed to test the influence of block breakage on the stability of the surrounding armour layer. Initially a revetment was constructed with ~5% of blocks either damaged or removed from the armour layer within eight block courses above and eight courses below the water level (CMB 5a, Figure 3.8). The damaged/removed blocks were either individual units or occasionally a pair of adjacent units. This revetment was tested with waves having a spectral peak period of 5 seconds and wave heights ranging up to the depth limited significant wave height (H_s~1.1 m). No displacement of blocks under the wave attack was observed (aside from displacement of blocks that were "damaged" prior to the test"), even blocks adjacent to "damaged" units. There was also no removal of secondary armour rock through the gaps in the armour layer. Pre and post-test photographs from this test are shown in Figure 5.4.
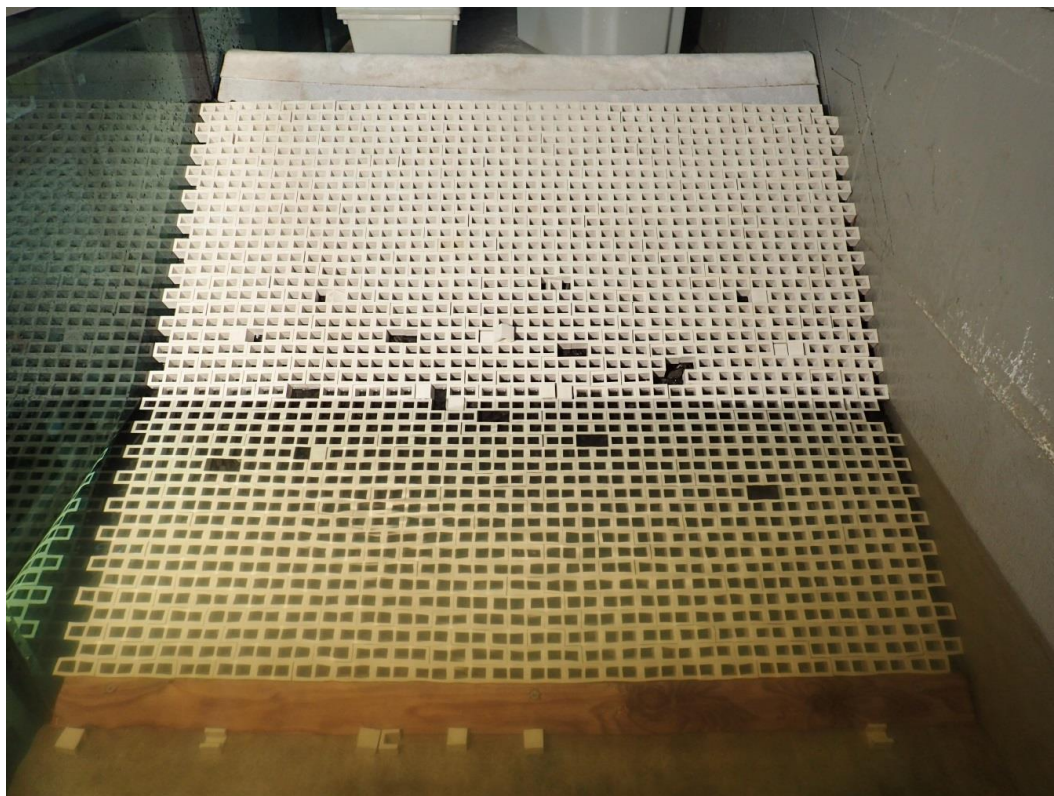
Figure 5.4: Pre and Post-Test Photos for CMB5a
(Hs~1.1 m, 5% Damaged Armour Blocks)

The revetment was then modified to have ~10% of the blocks either damaged or removed from the armour layer within eight (8) block courses above and eight (8) courses below the water level (CMB5b, Figure 3.9). This revetment was also tested with waves having a spectral peak period of 5 seconds and wave heights ranging up to the depth limited significant wave height (H_s~1.1 m).

With larger holes in the armour layer, waves with significant wave height as small as ~0.7 m were able to dislodge a small number of adjacent CMBs from the armour layer, as well as displacing significant quantities of secondary armour. Pre and post-test photos of this test are shown in Figure 5.5. More severe wave conditions with significant wave height of ~1.1 m resulted in additional ongoing displacement of CMBs adjacent to holes in the armour layer, removal of large quantities of secondary armour rock, and general fracturing/settlement of the CMB armour layer. Post-test photos from this more severe wave condition are shown in Figure 5.6.
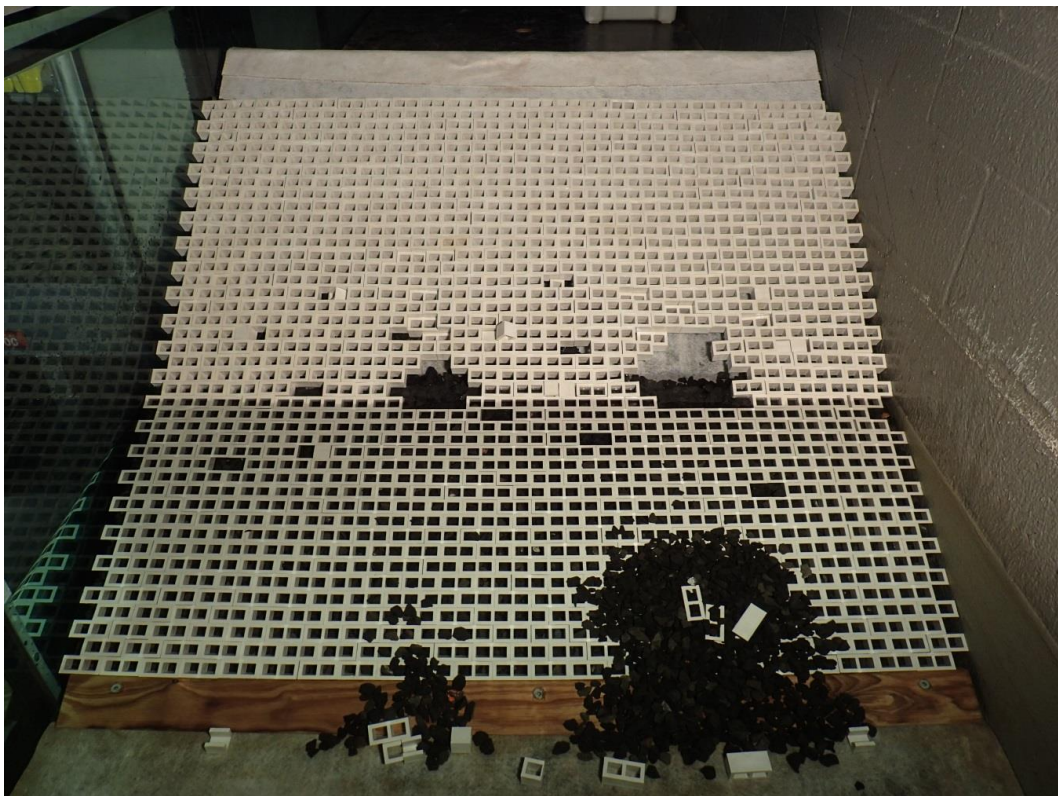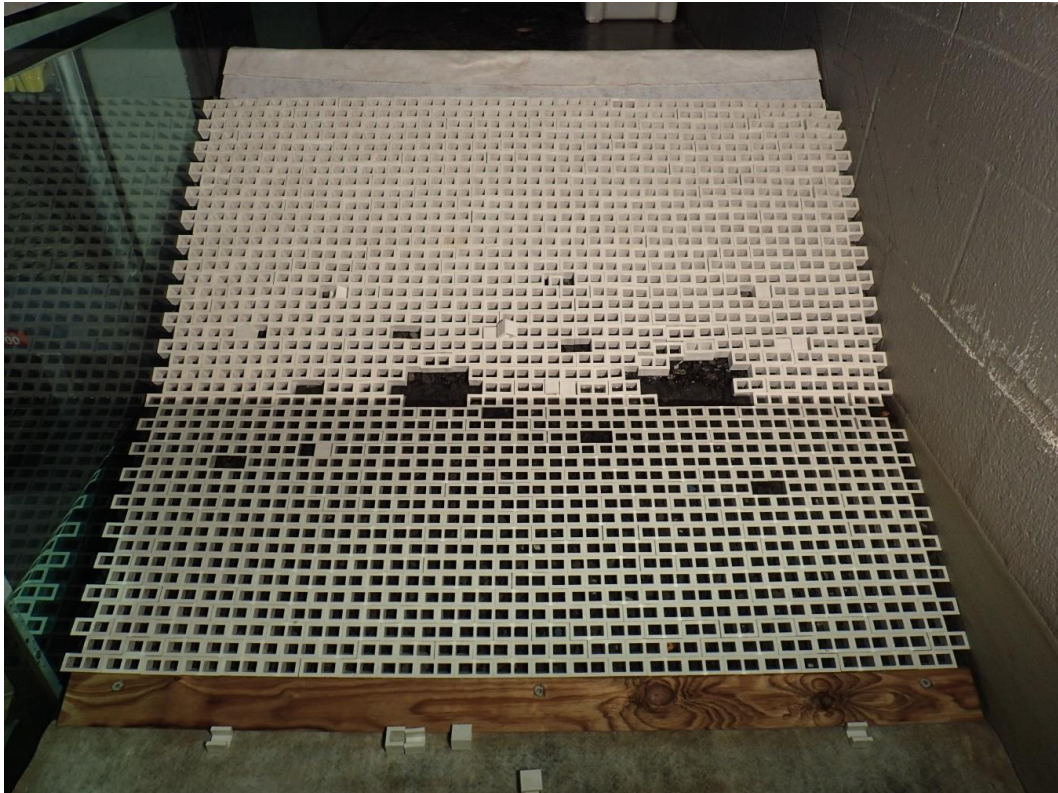
Figure 5.5: Pre and Post-Test Photos for CMB5b
(H$_s$~0.7 m, 10% Damaged Armour Blocks)
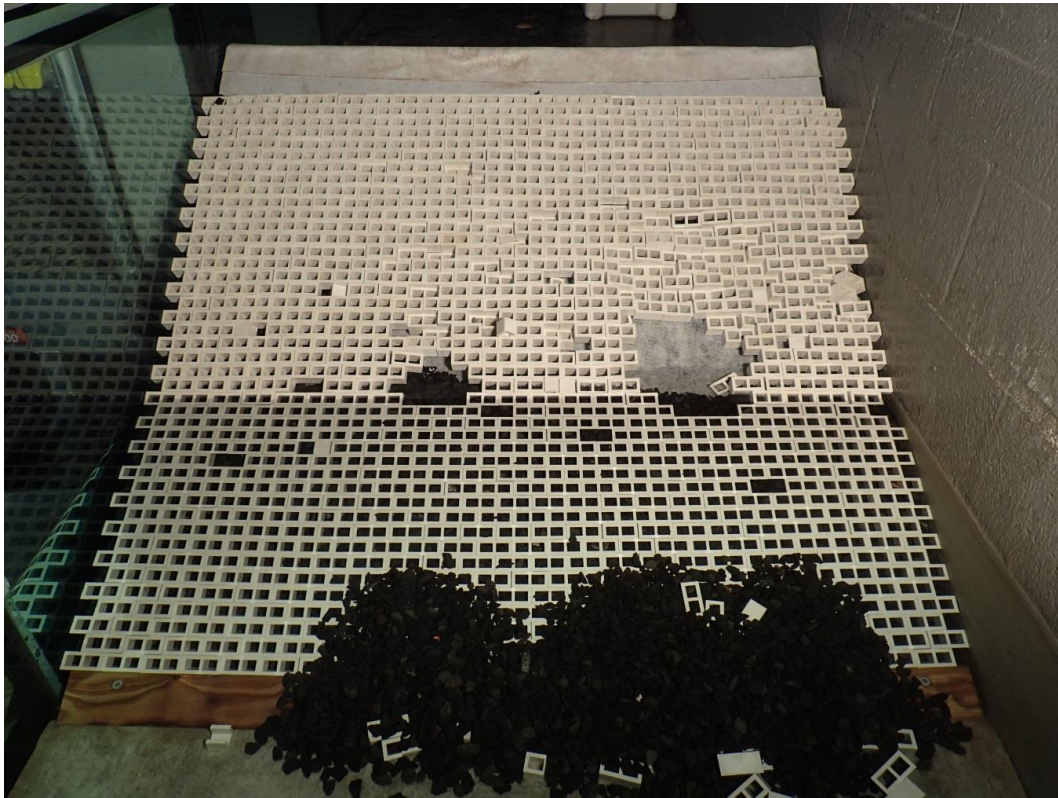
Figure 5.6: Post-Test Photos for CMB5b
(H_s~1.1 m, 10% Damaged Armour Blocks)

5.2   CMB Crest Armour Stability Characteristics

For most low-energy coastlines where a CMB revetment may be applicable, it is likely that the revetments would be relatively low crested and that some degree of wave overtopping would occur during storms. As such, the stability of CMBs placed at the crest of a revetment slope would likely differ when exposed to overtopping waves, compared with CMBs placed on the slope of a non-overtopped revetment.

A series of tests were undertaken with a lower crested revetment structure (CMB4) for 5 second period waves, to identify the upper limit of wave overtopping flows before the crest blocks became destabilised. The results are summarised in Table 5.1 and Figure 5.7. For average overtopping flow rates of up to 0.2 L/s/m, it was found that there was minimal damage sustained to the revetment crest (only minor damage that was potentially associated with a flume edge effect was observed). However, a slight increase in overtopping flow rate to 1.3 L/s/m resulted in significant displacement of crest blocks, with all blocks in the top row and several blocks in the second row completely displaced. It is likely that this test underestimated the observed damage, as in reality the displacement of crest blocks would likely coincide with erosion of the revetment substrate at the crest which would exacerbate destabilisation of blocks. This process was, however, not simulated in the model due to the presence of the fixed revetment core.

Table 5.1. CMB Crest Unit Stability for Overtopped Revetment

T$_p$ (s)	H$_s$ (m)	Ave. Over-topping rate (L/s/m)	Damage to Top 3 Block Courses	Crest Photo After Test
5	0.4	0.0	0%	
5	0.7	0.2	6%	
5	0.8	1.3	36%	
5	0.9	2.5	43%	
5	1.0	7.5	52%	
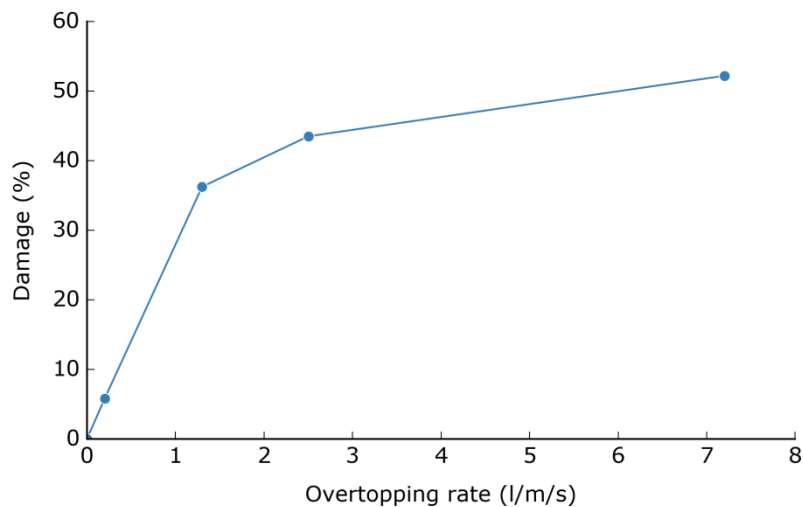
Figure 5.7. Damage to Top Three Block Courses on Revetment with Overtopping
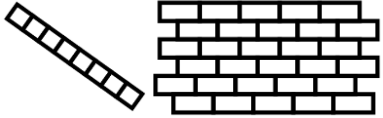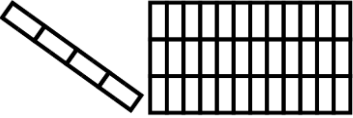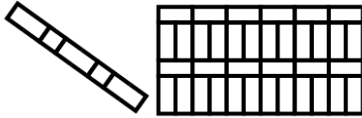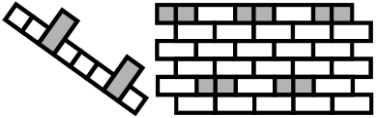
5.3   CMB Wave Runup Characteristics

Wave runup measurements were undertaken in parallel with armour stability measurements, to allow for analysis of runup characteristics for each CMB placement pattern, consistent with typical coastal engineering design methods (such as EurOtop, 2007). Table 5.2 and Figure 5.8 provide a summary of measured runup values for each CMB placement pattern tested (for the largest wave heights tested), with runup values on a smooth slope also reported for comparative

reference. The results indicate that there is very little difference in wave runup levels that occur with the various "in-plane" CMB placement patterns tested.

Additional tests were undertaken to investigate the reduction in wave runup that could be achieved by placing a small number of CMBs within the armour layer on their end as shown in Figure 3.10 for revetment CMB6 (long axis of block protruding outwards from armour layer and block holes facing cross-slope). While this armouring configuration does increase the cost of the armour layer (slightly higher number of blocks required), the results of the testing showed that for all three wave periods tested (3, 5, and 10 seconds), approximately 20% lower wave runup levels were achieved in comparison with a standard running bond placement pattern. These results are shown in Table 5.2 and Figure 5.8. A more detailed snapshot of the reduction in wave runup achieved with the "upstand" block placement pattern when compared to the standard "running bond" pattern is shown in Figure 5.9, which presents a time series of wave runup occurrences on the two tested revetments.

Table 5.2. Comparison of Runup Height for Different CMB Placement Patterns

T_p (s)	H_s (m)	$R_{u2\%}$ (m)				Smooth Slope
		CMB1	CMB2	CMB3	CMB6	
3	0.85	1.9	1.8	1.8	1.5	2.05
5	1.05	2.5	2.5	2.5	2.0	2.66
10	0.88	2.7	2.7	2.7	2.2	2.73

Note: CMB holes aligned in/out of slope surface
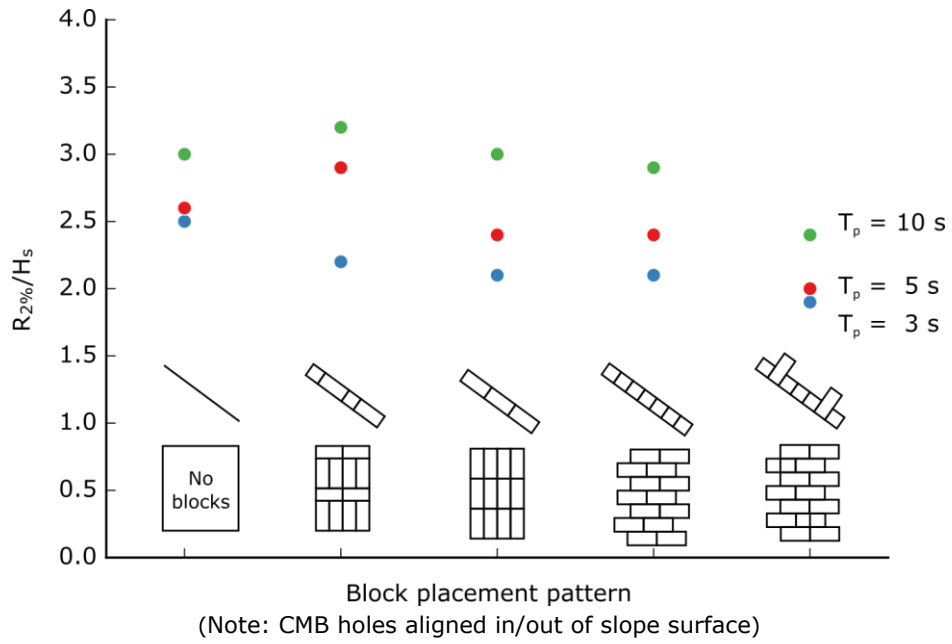
Figure 5.8: Comparison of Wave Runup with Various CMP Placement Configurations
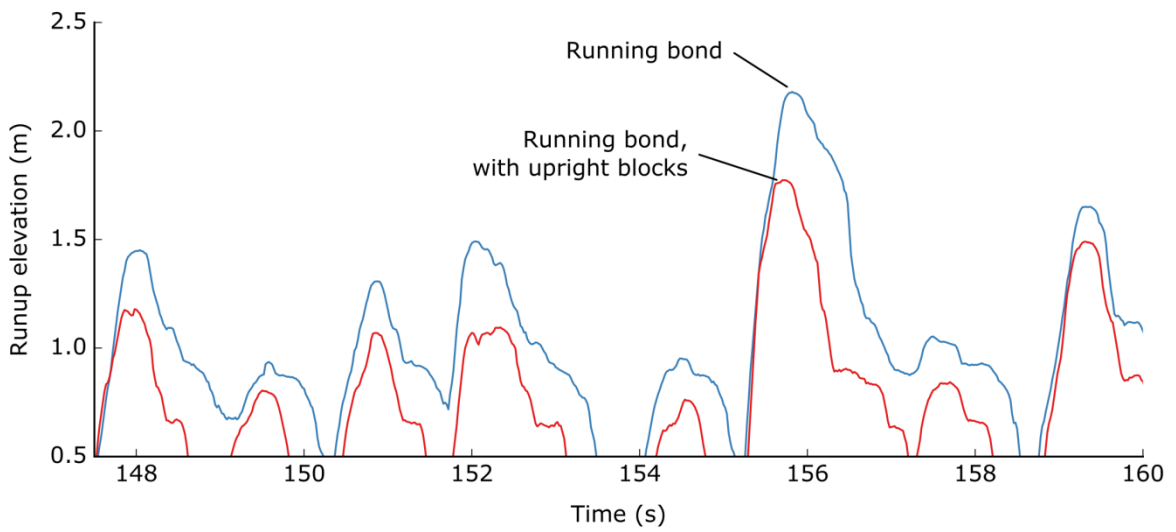
Figure 5.9: Example Comparison of Wave Runup Time-series for Upstand Blocks

6. Geotextile Sand-Filled Container Testing Results

6.1 GSC Slope Armour Stability Characteristics

Non-overtopped revetments constructed with two (2) different GSC placement patterns were both tested for wave periods (T_p) of 3, 5 and 10 seconds. The revetments were exposed to wave conditions with significant wave height increasing until complete failure of the GSC layer was achieved, in order to identify the upper limit stability threshold of the GSCs on the revetment slope.

Figure 6.1 shows the recorded stability results for revetment GSC1 (armoured with double layer GSCs placed with long axis shore-parallel). For this revetment it was identified that the GSCs could withstand waves with significant wave height up to 0.3-0.4 m without any bag displacement. Once the significant wave height was increased beyond 0.4 m the outer GSC layer on the revetment progressively failed with ongoing wave exposure. It was noted that the shorter period 3 second waves resulted in lower GSC stability, as the larger wave heights at this short period were actually breaking on the structure slope, as opposed to surging up the slope as was experienced for the longer period waves.
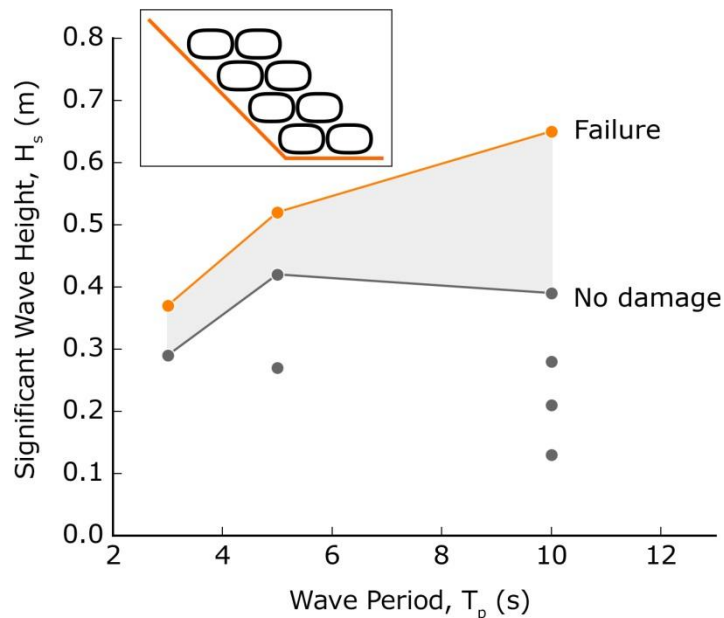
Figure 6.1: GSC1 Revetment Stability Results

Figure 6.2 shows the recorded stability results for revetment GSC2 (armoured with single layer GSCs placed with long axis shore-perpendicular). For this revetment it was identified that the GSCs could withstand waves with significant wave height up to ~0,5 m with only minor bag displacement. Once the significant wave height was increased to 0.6 m and beyond, the outer GSC layer on the revetment progressively failed with ongoing wave exposure. It was again noted that the shorter period 3 second waves resulted in slightly lower GSC stability compared with the longer period waves, due to the wave breaking intensity on the structure. It was also noted that this bag placement pattern with long axis running shore-perpendicular resulted in slightly higher stability, presumably due to the larger interface friction area between bags.

However, with a single layer or GSCs there is very little redundancy in the armour layer to cope with displaced bags compared with a double layer design.
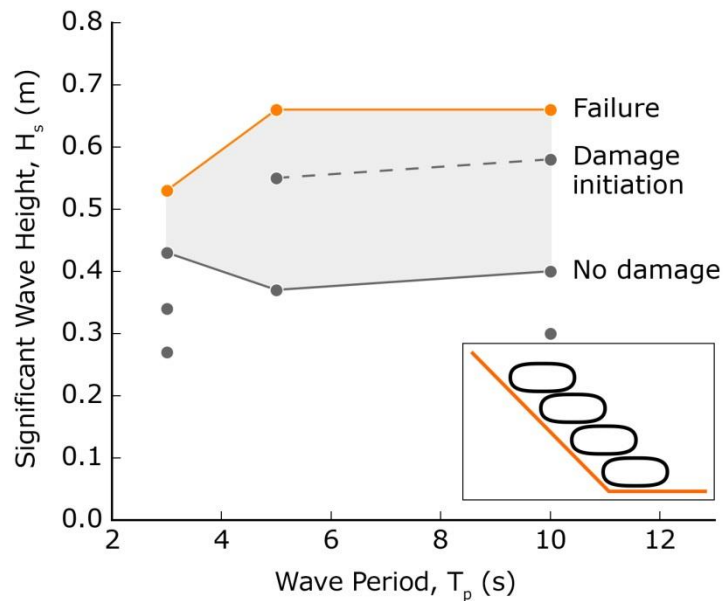
Figure 6.2: GSC2 Revetment Stability Results

6.2   GSC Crest Armour Stability Characteristics

For most low-energy coastlines where a GSC revetment may be applicable, it is likely that the revetments would be relatively low crested and that some degree of wave overtopping would occur during storms. As such, the stability of GSCs placed at the crest of a revetment slope would likely differ when exposed to overtopping waves, compared with GSCs placed on the slope of a non-overtopped revetment.

A series of tests were undertaken with a lower crested revetment structure (GSC3) for 5 second period waves, to identify the upper limit of wave overtopping flows before the crest bags became destabilised. A summary of the test results is provided in Table 6.1. A range of wave conditions with significant wave height up to 0.9 m and average overtopping rates up to 4 L/s/m were tested, and the GSCs at the crest of the revetment remained stable throughout all tests.

During these tests the slope of the revetment was mostly protected from wave attack to prevent the slope from failing at lower wave heights than the crest. Nevertheless during the final test, the upper slope area of the revetment failed prior to crest bags being displaced from overtopping.   Given the stability measurements for the non-overtopped GSC revetments (Section 6.1), these results indicate that it is likely that the GSC revetments would initially fail from slope armour instability rather than crest armour instability, unlike the CMB revetments.
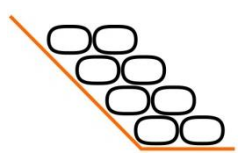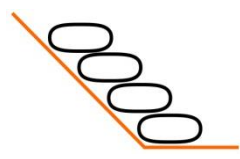
Table 6.1. GSC Crest Unit Stability for Overtopped Revetment

T_p (s)	H_s (m)	Ave. Over-topping Rate (L/s/m)	Damage to Top 3 Block Courses	Crest Photo After Test
5	0.4	0.0	0%	
5	0.5	0.0	0%	
5	0.6	0.1	0%	
5	0.7	0.6	0%	
5	0.8	1.2	0%	
5	0.9	1.9	0%	
5	0.9	4.1	0%	

6.3 GSC Wave Runup Characteristics

Wave runup measurements were undertaken in parallel with armour stability measurements, to allow for analysis of runup characteristics for both GSC placement patterns, consistent with typical coastal engineering design methods (such as EurOtop, 2007). Table 6.2 provides a summary of measured runup values for each CMB placement pattern tested.

Table 6.2. Comparison of Runup Height for Different GSC Placement Patterns.

T_p (s)	H_s (m)	$R_{u2\%}$ (m)	H_s (m)	$R_{u2\%}$ (m)
3	0.3	0.6	0.3	0.8
3	0.4	0.8	0.4	1.1
3			0.5	1.1
5	0.5	1.0	0.4	0.8
5			0.6	1.2
10	0.3	0.7	0.3	0.7
10	0.4	0.9	0.4	0.9
10			0.6	1.5
10	0.7	1.7	0.7	1.9

7. Conclusion

This physical modelling investigation has been undertaken to develop design guidance for a range of alternative/affordable coastal protection armour types, potentially suitable for application on low energy coastlines of Pacific Islands. In particular, the stability and runup characteristics of both small hand-placed geotextile sand-filled containers and concrete masonry building blocks when placed as revetment armouring, has been investigated. The investigation was undertaken using a 1:7.5 scale two-dimensional wave flume model in the 1.2 m wide flume at the Water Research Laboratory, UNSW Sydney. Both armouring systems were tested for a range of wave conditions expected to be experienced on low energy coastlines of Pacific Islands (such as lagoon coastlines of atolls), with a shallow flat bathymetry.

The stability of concrete masonry blocks in three alternative placement configurations was tested, and for all wave periods modelled (3 – 10 seconds), the blocks were found to be stable in waves up to almost 1 m significant wave height. This was considered the physical limit of wave height due to depth or steepness limitations on waves. It was only when the crest of the revetment was overtopped by waves that the crest armouring blocks became unstable. The threshold of block stability on the crest was investigated for a range of wave overtopping rates. Due to the potential that some blocks would be damaged during a storm, the impact of this damage on the stability of the overall armour layer integrity was also investigated.

The stability of small geotextile containers in two alternative placement configurations was tested, and for all wave periods modelled (3 – 10 seconds), the containers were found to have a stability limit of approximately 0.4 m significant wave height. Waves in excess of this height resulted in rapid displacement of the containers from the revetment face slope. The stability limit of geotextile containers placed on the crest of a revetment was also investigated for a range of overtopping flows, and unlike the concrete masonry blocks, the geotextile containers were stable in relatively high flows (up to 4 L/s/m was tested).

8. References

Blacka, M., Carley, J., Cox, R., Hornsey, W. and Restall, S. (2007) *Field Measurements of Full Sized Geocontainers*, Proceedings of the Coasts and Ports Conference, Engineers Australia

Coghlan, I., Carley, J., Cox, R., Blacka, M., Mariani, A., Restall, S., Hornsey, W. and Sheldrick, S. (2009) *Two-Dimensional Physical Modelling of Sand Filled Geocontainers for Coastal Protection*, Proceedings of the Coasts and Ports Conference, Engineers Australia

EurOtop (2007) *Wave Overtopping of Sea Defences and Related Structures*, Assessment Manual

PRIF (2016) *Affordable Coastal Protection,* Desktop Review Report

PRIF (2016) *Request for Quotation, Terms of Reference*, TA-8345 REG: Training/Seminars Studies Budget (Affordable Coastal Protection Project)

Appendix A: Geotextile Scaling Considerations

A detailed analysis of GSC scaling for physical modelling was presented in Coghlan *et al.* (2009), for a 1:8 scale model of both 0.75 m³ and 2.5³ GSCs. With a 1:7.5 length scale adopted for this investigation of 40 kg GSCs, the majority of the key scaling considerations are directly relevant and discussed below.

Geotextile Container Shape – Tensile Strength

The shape of the sand filled GSCs was an important consideration in the design of the physical model, as their stability under wave attack is affected by how well they deform and fit together. It was important to generate similar cross-sectional shape characteristics as the real-world full scale bags measured in the field by Blacka et *al.* (2007). The tensile strength of the bag fabric was previously determined to be a major contributing parameter to GSC shape (Coghlan *et al.,* 2009). Tensile force was defined broadly at any position in a geosynthetic shell by Leshchinsky *et al.* (1996) as:

$$T_f = P\,r$$

Where: T_f: the tensile force in the geotextile (kN/m)
                 P: the pressure on the geotextile (kPa)
                 r: the local radius in a vertical cross-section through the centre (m)

Pilarczyk (2000) showed that the Leshchinsky *et al.* (1996) equation may be scaled as:

$$T_{f\,R} = L_R^2$$

Where: $T_{f\,R} = \dfrac{T_{f\,PROTOTYPE}}{T_{f\,MODEL}}$ $L_R = \dfrac{L_{PROTOTYPE}}{L_{MODEL}}$

Since a length scale, L_R, of 7.5 was selected for the modelling, the theoretical ideal tensile strength of the model material will be 1/7.5² of the prototype value (kN/m). However, given the finite number of geotextiles to select from, it is not possible to select a product that exactly matches this requirement. Instead the geotextile fabric used in the modelling was as close as possible, but slightly stiffer than the ideal fabric so that the modelling results were conservative.

Geofabrics Australasia provide tensile strength characteristics of the range of fabrics typically used for GSCs (Table A.1). While it is not known exactly which fabric would be used for full scale 40 kg GSCs, it can be seen from this data that the FT150 fabric previously used in model testing by Coghlan *et al.* (2009), was again the most suitable for this model testing in terms of having the closest (but slightly higher) tensile strength characteristics to the full scale fabrics. Geotextile FT150 had a tensile strength too strong by factor of 7 to 14, however, this was the thinnest suitable material available. Most importantly, for correct reproduction of prototype behaviour, the shape of the geocontainers was observed to be similar to the prototype installations justifying the model geotextile material choice.

Table A.1: Tensile Strength Characteristics of Texcel Geotextile Fabrics (Geofabrics; Coghlan *et al.* 2009)

Fabric Type	Prototype Tensile Strength (KN/m) MD/XD	Model Scale Tensile Strength (KN/m) MD/XD
400R	16/16	0.28/0.28
600R	26.5/26.5	0.47/0.47
900R	37/37	0.66/0.66
1200R	59/59	1.05/1.05
FT150	4.08/6.55	

8.1.1.1 Geotextile Hydraulic Conductivity

For the model geotextile chosen on the basis of tensile strength (FT150), the material hydraulic conductivity, K, was also checked.

Ideally, $K_R = \dfrac{K_{PROTOTYPE}}{K_{MODEL}} = L_R^{0.5}$

$$K_{MODEL\,ideal} = \dfrac{K_{PROTOTYPE}}{L_R^{0.5}}$$

K has been quoted based on the test method outlined in AS 3706.9 (2001), where the flow rate under 100 mm of head is measured across a square metre of geotextile. As the thickness of the geotextile is reduced, the relative influence of entry and exit losses increase, and so K_{MODEL} was expressed as $K_{EFFECTIVE}$, rather than as a *K* that does not consider such losses.

Due to the relatively small thickness of the geotextile to the much wider extent of the filler sand, no significant scaling errors are likely provided $K_{MODEL\,(EFFECTIVE)}$ > $K_{MODEL\,ideal}$.

For the length scale of 7.5, K_R is 2.74. Application of the Darcy equation (Fitts, 2002) yields the ideal model material in Table A.2.

Table A.2: Scaling of Material by Hydraulic Conductivity (7.5 Scale)

Material	Prototype (800RX)	Ideal Model Material (7.5 scale)	Selected Material: FT150
	Flow Rate Under 100 mm Head per square metre of Geotextile Material		
Hydraulic Conductivity, $K_{EFFECTIVE}$ (L/m^2/s)	62	22.6	300

Since $K_{m\,(EFFECTIVE)}$ > $K_{m\,ideal}$ the material was considered appropriate for testing. Geotextile FT150 was more conductive than the ideal material by a factor of approximately 13. This was considered to be tolerable in the model.

8.1.1.2 Geotextile Fabric to Fabric Friction

Geotextile fabric to fabric friction is important for replicating the load required to dislodge GSCs from the armour layer. This has been clearly observed in field applications where the extra friction provided in the composite geotextiles (i.e. vandal resistant) results in increased but unquantified stability. While friction data is available for the common prototype 800RX material, no suitable data was available for the model material, and as such no further consideration of the influence of container to container friction was possible.

8.1.1.3 Hydraulic Conductivity of Filler Sand

Non-cohesive sand materials typically considered for fill material in GSCs have an approximate porosity of 40 per cent. It was important to select a model filler sand with as near to the correct scaling as possible for hydraulic conductivity:

$$K_R = \frac{K_{PROTOTYPE}}{K_{MODEL}} = L_R^{0.5}$$

Sand grain sizing was undertaken based on the Kozeny-Carmen equation (Fitts, 2002):

$$K = \left(\frac{\rho_w g}{\mu}\right)\left(\frac{n^3}{(1-n)^2}\right)\left(\frac{(d_{50})^2}{180}\right)$$

Where: K = saturated hydraulic conductivity (m/s)

$\left(\frac{\rho_w g}{\mu}\right)$ = the unit weight of water/viscosity of water (ms)$^{-1}$

n = porosity (ratio of non-solid volume to total volume)
d_{50} = median grain diameter (m)

Such that: $d_{50R} = \dfrac{d_{50MODEL}}{d_{50PROTOTYPE}} = K_R^{0.5} = L_R^{0.25}$

So, the median grain diameter of the filler sand scales with $L_R^{0.25}$. Assuming the prototype sand has a d_{50} of 0.3-0.4 mm, model sand at 7.5 scale would ideally have a d_{50} of 0.18-0.24 mm.

WRL acquired "Anna Bay" sand for filling the model GSCs; this is a fine grained natural marine sand with a d_{50} of 0.22 mm and was considered the most suitable material readily available for modelling. For this grain size the hydraulic conductivity of the selected geotextile was much higher than the filler sand, as preferred. A sediment grading of a sample of "Anna Bay" sand is provided in Appendix B.

Appendix B: GSC Sand Fill Specifications

Fill sand for the model geotextile containers was sourced from Anna Bay, NSW due to its fine grained nature. Table B.1 provides grading specifications for the fill sand.

Table B.1: Grading Properties for Model GSC Fill Sand

Sieve Size (µm)	Cumulative % Retained (%)
355	0
250	4.2
180	77.6
125	99.3
90	99.9
<90	100
205	D_{50}

Appendix C: Tabulated Test Results

C.1 Tabulated Concrete Masonry Block Testing Results

Table C.1: CMB Slope Armour Stability and Runup Test Results

Revetment Reference	Armouring	Wave Period, T_p (s)	Upper Wave Height, H_s (m)	Runup Height, $R_{2\%}$ (m)	Results
CMB1	Long axis shore parallel	3	0.9	1.9	Armour stable, maximum wave steepness achieved
		5	1.1	2.5	Armour stable, depth limited waves achieved offshore
		10	0.9	2.7	Armour stable, wave machine capacity reached
CMB2	Long axis shore perpendicular	3	0.8	1.9	Armour stable, maximum wave steepness achieved
		5	1.0	2.5	Armour stable, depth limited waves achieved offshore
		10	0.9	2.6	Armour stable, wave machine capacity reached
CMB3	Alternating courses of shore parallel and shore perpendicular	3	0.8	1.8	Armour stable, maximum wave steepness achieved
		5	0.9	2.5	Armour stable, depth limited waves achieved offshore
		10	0.8	2.6	Armour stable, wave machine capacity reached
Smooth Slope	No armour	3	0.8	2.0	Maximum wave steepness achieved
		5	1.0	2.7	Depth limited waves achieved offshore
		10	0.8	2.8	Wave machine capacity reached

Table C.2: CMB Crest Armour Stability Test Results

Revetment Reference	Armouring	Wave Period, T_p (s)	Upper Wave Height, H_s (m)	Ave. Overtopping Rate, Q (L/s/m)	Results
CMB4	Long axis shore parallel	5	0.4	0.0	0% of blocks in top 3 rows displaced
			0.7	0.2	6% of blocks in top 3 rows displaced
			0.8	1.3	36% of blocks in top 3 rows displaced
			0.9	2.5	43% of blocks in top 3 rows displaced
			1.0	7.2	52% of blocks in top 3 rows displaced

Table C.3: Additional CMB Armour Stability and Runup Test Results

Revetment Reference	Armouring	Wave Period, T_p (s)	Upper Wave Height, H_s (m)	Runup Height, $R_{2\%}$ (m)	Results
CMB5a	Long axis shore parallel (5% "damaged" units)	5	1.1	N/A	Armour units stable. No extraction of 2ndry armour through "damage" holes in block layer
CMB5b	Long axis shore parallel (10% "damaged" units)	5	1.1	N/A	Small percentage of blocks adjacent to "damage" holes were displaced. Significant erosion/displacement of 2ndry armour resulting settlement/fracturing of CMB matrix
CMB6	Long axis shore parallel with upstand blocks	5	1.0	2.0	Armour stable, depth limited waves achieved offshore

C.2 Tabulated Geotextile Sand-Filled Container Testing Results

Table C.4: GSC Slope Armour Stability and Runup Test Results

Revetment Reference	Armouring	Wave Period, T_p (s)	Wave Height, H_s (m)	Runup Height, $R_{2\%}$ (m)	Results
GSC1	Double layer long axis shore parallel	3	0.3	0.6	No GSCs displaced
		3	0.4	0.8	Initial and ongoing GSC displacement
		5	0.3	-	No GSCs displaced
		5	0.4	-	No GSCs displaced
		5	0.5	1.0	Initiation of GSC displacement
		5	0.6	-	Ongoing GSC displacement
		10	0.1	0.2	No GSCs displaced
		10	0.2	0.4	No GSCs displaced
		10	0.3	0.7	No GSCs displaced
		10	0.4	0.9	No GSCs displaced
		10	0.7	1.7	Initial and ongoing GSC displacement
GSC2	Single layer long axis shore perpendicular	3	0.3	0.7	No GSCs displaced
		3	0.3	0.8	No GSCs displaced
		3	0.4	1.1	No GSCs displaced
		3	0.5	1.1	Initial and ongoing GSC displacement
		5	0.4	0.8	No GSCs displaced
		5	0.6	1.2	Initiation of GSC displacement
		5	0.7	-	Ongoing GSC displacement
		10	0.3	0.7	No GSCs displaced
		10	0.4	0.9	No GSCs displaced
		10	0.6	1.5	Initiation of GSC displacement
		10	0.7	1.9	Ongoing GSC displacement

Table C.5: GSC Crest Armour Stability Test Results

Revetment Reference	Armouring	Wave Period, T_p (s)	Wave Height, H_s (m)	Ave. Overtopping Rate, Q (L/s/m)	Results
GSC3	Double layer long axis shore parallel	5	0.4	0.0	0% of crest bags displaced
			0.5	0.0	0% of crest bags displaced
			0.6	0.1	0% of crest bags displaced
			0.7	0.6	0% of crest bags displaced
			0.8	1.2	0% of crest bags displaced
			0.9	1.9	0% of crest bags displaced
			0.9	4.1	0% of crest bags displaced

Appendix D: GSC Stability Comparison with Coghlan *et al.* (2009)

To check the consistency of the results from this modelling investigation with previous investigations of geotextile sand filled container stability, a comparison was made with the results from the Coghlan *et al*. (2009) paper. Coghlan *et al*. (2009) investigated and presented results for the stability of 0.75 m^3 GSCs under wave attack for 5, 10 and 15 second period waves. The results from the current investigation were rescaled using a geometric length scale of 1:23.71, such that the model bags were equivalent to the 0.75 m^3 bags reported in Coghlan *et al.* (2009). A comparison of the stability results from the two investigations is provided in Figure D.1.

It can be seen from the comparison that when re-scaled, the results from both investigations indicate that damage to a 0.75 m^3 GSC armoured revetment will occur at a similar magnitude of wave height. The slight differences in stability reported between the investigations are expected to be a result of differences in experimental setup:

- The revetments tested in Coghlan et al., (2009) were constructed with a permeable sand core in comparison to the impermeable core assumed for the current investigation;

- The testing undertaken in Coghlan *et al.,* (2009) used a 1V:5, 1V:10 or 1V:20 beach slope seaward of the test structure, in comparison with the flat bathymetric profile adopted for this investigation. This will have resulted in more severe wave breaking on the revetment slope at longer wave periods, compared with the current investigation.
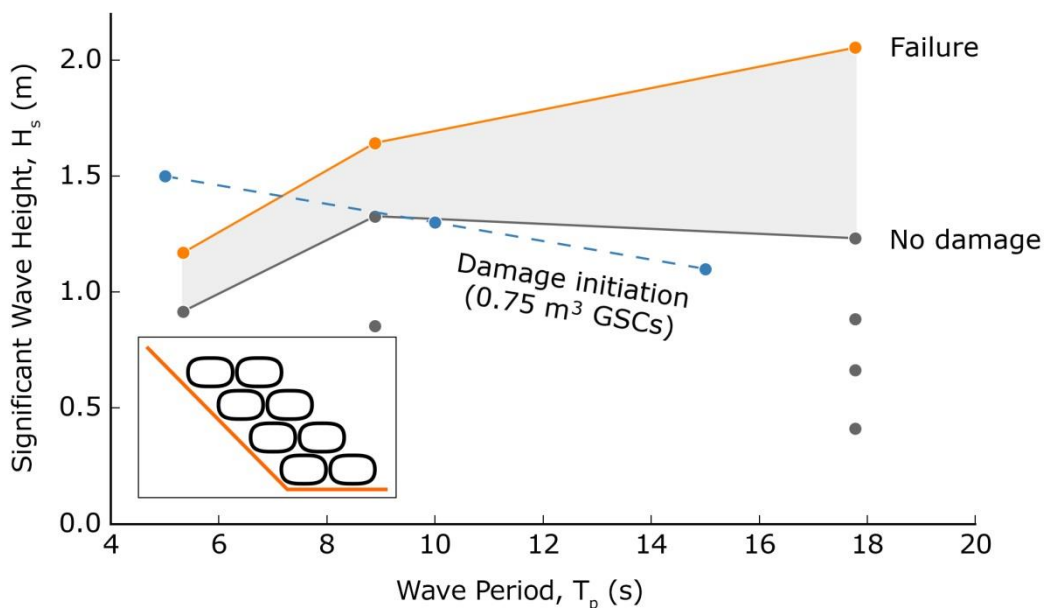

Figure D.1: Comparison of GSC stability Results with Previous Investigations